

RESEARCH

Open Access



Multi-omics analysis reveals CMTR1 upregulation in cancer and roles in ribosomal protein gene expression and tumor growth

Ion John Campeanu¹, Yuanyuan Jiang¹, Hilda Afisllari¹, Sijana Dzinic^{1,2}, Lisa Polin^{1,2} and Zeng-Quan Yang^{1,2*}

Abstract

Background CMTR1 (cap methyltransferase 1), a key nuclear mRNA cap methyltransferase, catalyzes 2'-O-methylation of the first transcribed nucleotide, a critical step in mRNA cap formation. Previous studies have implicated CMTR1 in embryonic stem cell differentiation and immune responses during viral infection; however, its role in cancer biology remains largely unexplored. This study aims to elucidate CMTR1's function in cancer progression and evaluate its potential as a novel therapeutic target in certain cancer types.

Methods We conducted a comprehensive multi-omics analysis of CMTR1 across various human cancers using TCGA and CPTAC datasets. Functional studies were performed using CRISPR-mediated knockout and siRNA knockdown in human and mouse basal-like breast cancer models. Transcriptomic and pathway enrichment analyses were carried out in CMTR1 knockout/knockdown models to identify CMTR1-regulated genes. In silico screening and biochemical assays were employed to identify novel CMTR1 inhibitors.

Results Multi-omics analysis revealed that CMTR1 is significantly upregulated at the mRNA, protein, and phosphoprotein levels across multiple cancer types in the TCGA and CPTAC datasets. Functional studies demonstrated that CMTR1 depletion significantly inhibits tumor growth both in vitro and in vivo. Transcriptomic analysis of CMTR1 knockout cells revealed that CMTR1 primarily regulates ribosomal protein genes and other transcripts containing 5'Terminal Oligopyrimidine (TOP) motifs. Additionally, CMTR1 affects the expression of snoRNA host genes and snoRNAs, suggesting a broader role in RNA metabolism. Mechanistic studies indicated that CMTR1's target specificity is partly determined by mRNA structure, particularly the presence of 5'TOP motifs. Finally, through in silico screening and biochemical assays, we identified several novel CMTR1 inhibitors, including N97911, which demonstrated in vitro growth inhibition activity in breast cancer cells.

Conclusions Our findings establish CMTR1 as an important player in cancer biology, regulating critical aspects of RNA metabolism and ribosome biogenesis. The study highlights CMTR1's potential as a therapeutic target in certain cancer types and provides a foundation for developing novel cancer treatments targeting mRNA cap methylation.

Keywords RNA methyltransferase, CMTR1, Ribosomal proteins, Small molecule inhibitor

*Correspondence:

Zeng-Quan Yang
yangz@karmanos.org

¹Department of Oncology, Wayne State University School of Medicine,
Detroit, MI, USA

²Molecular Therapeutics Program, Barbara Ann Karmanos Cancer
Institute, Detroit, MI, USA



© The Author(s) 2025. **Open Access** This article is licensed under a Creative Commons Attribution-NonCommercial-NoDerivatives 4.0 International License, which permits any non-commercial use, sharing, distribution and reproduction in any medium or format, as long as you give appropriate credit to the original author(s) and the source, provide a link to the Creative Commons licence, and indicate if you modified the licensed material. You do not have permission under this licence to share adapted material derived from this article or parts of it. The images or other third party material in this article are included in the article's Creative Commons licence, unless indicated otherwise in a credit line to the material. If material is not included in the article's Creative Commons licence and your intended use is not permitted by statutory regulation or exceeds the permitted use, you will need to obtain permission directly from the copyright holder. To view a copy of this licence, visit <http://creativecommons.org/licenses/by-nc-nd/4.0/>.

Background

The mRNA cap, a highly methylated modification at the 5' end of RNA polymerase II (RNA Pol II)-transcribed RNAs, plays multiple critical roles in eukaryotic gene expression [1–7]. It protects RNA from degradation both during transcription and in the cytoplasm, recruits protein complexes involved in RNA processing, nuclear export, and translation initiation, and marks cellular mRNA as 'self' to prevent degradation by the innate immune system [1–7]. The formation and methylation of the cap structure are catalyzed by a set of specialized enzymes. During the early stages of transcription, RNGTT (RNA guanylyltransferase and triphosphatase) attaches the inverted guanosine cap to the first transcribed nucleotide via a triphosphate bridge [1, 2, 7, 8]. Subsequently, a series of cap methyltransferases including RNMT (RNA guanine-7 methyltransferase), CMTR1 (cap methyltransferase 1), CMTR2 (cap methyltransferase 2), and/or PCIF1 (phosphorylated CTD interacting factor 1) methylate specific sites on the guanosine cap and the first two transcribed nucleotides [1–7]. This process protects and stabilizes mRNA while serving as a crucial regulatory mechanism for gene expression, influencing various cellular processes including development, differentiation, and disease progression.

CMTR1 and CMTR2, which contain a unique Rossmann fold methyltransferase domain known as Ftsj, catalyze 2'-O-methylation of the first and second transcribed nucleotides, respectively [9–14]. However, CMTR1 and CMTR2 contain distinct functional domains flanking their Ftsj methyltransferase domains [12]. Additionally, CMTR1 in mammals, including humans, is predominantly nuclear, while CMTR2 is primarily cytoplasmic [13]. Notably, CMTR1 interacts directly with RNA polymerase II via its WW domain, preferentially binding to Ser-5 phosphorylated C-terminal domains (CTDs) [15, 16]. This interaction allows CMTR1 to be recruited effectively to transcription start sites, correlating with RNA polymerase II abundance. Recent studies also revealed that CMTR1 has gene-specific impacts on transcript abundance and plays a significant role in embryonic stem cell differentiation, particularly in maintaining expression of histone and ribosomal protein genes [17]. As *CMTR1* is a known interferon-stimulated gene, it also plays roles in immune-mediated pathways during viral infection [16, 18–20]. CMTR1 inhibition provides strong protection against infection by multiple influenza A strains, and synergizes with the viral endonuclease inhibitor baloxavir, which blocks influenza A infection by preventing cap snatching [18]. Thus, CMTR1 functions as a key RNA methyltransferase, playing crucial roles in RNA metabolism and gene regulation, among its many functions.

Dysregulation of RNA methyltransferases has been linked to various human diseases, including cancer

[21–29]. Previously, we employed an unbiased approach to investigate genetic alterations in over 50 methyltransferases across a large panel of human cancers. This analysis led to the identification of FTSJ3, an rRNA 2'-O-methyltransferase, as an important regulator of breast cancer progression [22]. Among five mRNA cap-related enzymes, over-expression of RNMT has been observed in various cancers and correlated with patient outcomes [30]. Deletion of RNMT reduces proliferation and increases apoptosis, particularly in breast cancer cells harboring *PIK3CA* (phosphatidylinositol-4,5-bisphosphate 3-kinase catalytic subunit alpha) mutations [31]. A recent study revealed that PCIF1 is a critical regulator of CD8+ T cell antitumor immunity, primarily by modulating CD8+ T cell ferroptosis and activation [32]. CMTR1 has also been implicated in cancer progression, with evidence emerging from some cancer types. For instance, *CMTR1-ALK* fusions have been reported in a lung cancer patient with crizotinib resistance [33]. Furthermore, CMTR1 promotes cancer growth via regulation of STAT3 (signal transducer and activator of transcription 3) expression in colorectal cancer, and a recent study found that CMTR1 drives gastric cancer progression by facilitating *CD44* alternative splicing [34, 35]. However, despite these observations, the genomic and transcriptomic alterations of CMTR1 and its functional roles in human cancer remain largely unexplored.

In this study, we aimed to understand the genetic and transcriptomic patterns, as well as the clinical significance, of cap methyltransferases—focusing primarily on CMTR1—by employing an unbiased multi-omics approach across a large dataset of various human cancers. We used genetic approaches to inhibit CMTR1 and identified its downstream targets in both human and mouse cancer models. Additionally, we explored in silico screening and biochemical assays to identify novel CMTR1 inhibitors. Our results highlight the therapeutic potential of targeting CMTR1 in certain cancer types.

Methods

Bioinformatic data collection and analyses

Normalized RNA-sequencing data from 11,069 TCGA (The Cancer Genome Atlas) samples, including 737 normal samples, were downloaded from the GDC portal (<https://gdc.cancer.gov>). Normalized proteomics, phosphoproteomics, and/or acetylproteome data from CPTAC (Clinical Proteomic Tumor Analysis Consortium) samples, as well as clinical information, were downloaded from LinkedOmics (<http://linkedomics.org>) and cProSite (<https://cprosite.ccr.cancer.gov/>) [36–38]. Tumor types containing at least 10 paired TCGA or CPTAC normal samples were selected to calculate the mRNA and protein expression differences between tumor and normal samples. Statistical differences in

gene, protein, or modified protein levels were calculated by Mann-Whitney U test or Brown-Forsythe and Welch ANOVA using GraphPad Prism 10 or R. Cancer dependency scores for CMTR1 and CMTR2 were downloaded from the DepMap website (<https://depmap.org/portal/>) using the 24Q2 dataset [39]. For RNA-seq data (GSE141171) analysis of A549 CMTR1 wild-type (WT) and knockout (KO) cells with or without interferon (IFN) treatment, differential gene expression was performed using GREIN (<http://www.ilincs.org/apps/grein/?gse=>) [40].

CRISPR-mediated CMTR1 knockout and siRNA CMTR1 knockdown

The CRISPR-mediated *Cmtr1* knockout 4T1 mouse breast cancer model was generated by Synthego. Both wild-type and *Cmtr1*-KO 4T1 cells were cultured in RPMI supplemented with 10% fetal bovine serum (FBS). Briefly, we designed a single guide RNA (sgRNA) with the target sequence AUUCGCUUCUGUUUCUUGA G, to knock out mouse *Cmtr1*. This sgRNA was complexed with SpCas9 (*Streptococcus pyogenes* Cas9) to create a ribonucleoprotein (RNP). The RNP was then introduced into the 4T1 cells using optimized electroporation settings. Subsequently, we employed PCR and Sanger sequencing to confirm the successful knockout of *Cmtr1* in the 4T1 cells. The *Cmtr1* protein levels in 4T1 CRISPR control and *Cmtr1*-KO cells were also measured by Western blotting with anti-CMTR1 antibody (Bethyl catalog number A300-304 A). A human basal-like breast cancer line MDA-MB-436 was cultured in DMEM supplemented with 10% FBS. For siRNA knockdown of CMTR1 in the MDA-MB-436 model, cells were plated in 6-well plates (for RNA and protein collection) or 24-well plates (for survival assay) at proportional concentrations. Cells were then transfected using Sigma-Aldrich MISSION esiRNAs (60 nM) targeting CMTR1 or control eGFP according to the manufacturer's protocol. RNA was collected 48 h after transfection, while protein was collected 72–96 h post-transfection. Cell proliferation and/or survival in CRISPR-mediated *Cmtr1* knockout 4T1 cells and siRNA CMTR1 knockdown MDA-MB-436 cells were measured using a CellTiter-Blue Cell Viability Assay Kit and crystal violet staining.

Soft agar assay

Soft agar assays were performed as previously described [41]. Briefly, dishes were coated with a 1:1 mixture of the appropriate 2× medium for the 4T1 cell line and 1% Bacto agar. Cells were plated at 1×10^4 per well, fed three times per week for 3 to 4 weeks, stained overnight with 500 µg/mL p-iodonitrotetrazolium violet (Sigma, St. Louis, MO), and counted using an Oxford Optronix Gel-Count colony counter.

Analysis of 4T1 RNA-seq data

For RNA-seq of 4T1 WT and *Cmtr1*-KO cells, poly(A) RNA sequencing libraries were prepared following Illumina's TruSeq-stranded-mRNA sample preparation protocol. RNA integrity was checked with an Agilent Technologies 2100 Bioanalyzer. Poly(A) tail-containing mRNAs were purified using oligo-(dT) magnetic beads with two rounds of purification. Quality control analysis and quantification of the sequencing libraries were performed using an Agilent Technologies 2100 Bioanalyzer High Sensitivity DNA Chip. Paired-end sequencing was performed on Illumina's NovaSeq 6000 sequencing system. We used HISAT2 to map reads to the mouse genome (mm10). Differentially expressed mRNAs were identified using the R package edgeR. Pathway analysis was performed with Enrichr using the KEGG 2019 Mouse or KEGG 2021 Human datasets (<https://maayanlab.cloud/Enrichr/>) [42, 43].

RNA preparation and semiquantitative PCR reactions

To assess gene expression changes at the mRNA level, RNA was extracted from 4T1 and MDA-MB-436 cell lines using a RNeasy Plus Mini Kit (QIAGEN). For experiments examining snoRNA expression changes via PCR, RNA was extracted using a miRNasy Kit (QIAGEN), which isolates total RNA, including microRNAs and other small RNA species. The RNA was mixed with qScript cDNA SuperMix (Quanta Biosciences, Gaithersburg, MD, USA) and converted to cDNA through reverse transcription (RT). The resulting cDNA was then used for real-time PCR reactions with the following settings: 50 °C for 2 min, 95 °C for 10 min, 40 or 45 cycles of 95 °C for 15 s, 60 °C for 30 s, 72 °C for 30 s, followed by 72 °C for 10 min. Sequences of a set of primers for genes and snoRNAs were obtained from PrimerBank or designed using Primer3 tool [44, 45]. *PUM1* (human) or *Gapdh* (mouse) primer sets were used as controls.

In vivo tumor growth

All animal studies were approved by the Wayne State University Institutional Animal Care and Use Committee. A total of 2×10^6 WT or *Cmtr1*-KO 4T1 cells were injected into the mammary fat pads of female BALB/c mice. Tumor size was measured with calipers two to three times per week, and mice were euthanized when the tumor burden exceeded 1,500 mg. Bilateral tumor volumes from individual mice were used to calculate the growth of WT and *Cmtr1*-KO tumors using the formula volume (mg) = $L \times w^2/2$ where length (L, mm) and width (w) were determined by caliper measurements.

Virtual and biochemical screening of CMTR1 inhibitor

The crystal structure of human CMTR1 (PDB: 4N49) at 1.9 Å resolution was prepared with UCSF Chimera for

virtual screening against three NCI compound sets: the Diversity Set, Mechanistic Set, and Natural Products Set [46, 47]. Chemical and biological data for these NCI compounds are available at https://dtp.cancer.gov/dtps_tandard/dwindex/index.jsp. For MTiOpenScreen Vina docking, the grid center coordinates for the SAM binding pocket of 4N49 were set to $(x, y, z) = (8.9, 20.8, 16.6)$, with a search space size of $20 \text{ \AA} \times 20 \text{ \AA} \times 20 \text{ \AA}$. The MTiOpenScreen screening was repeated three times, and compounds shared across all three runs were further analyzed using DataWarrior, PyMOL, and UCSF Chimera. Based on virtual screening scores and predicted physicochemical properties, 18 compounds were selected for future validation using Bio-Layer Interferometry (BLI) assays, which were performed according to the manufacturer's protocol.

Results

Differential expression and phosphorylation of CMTR1 and CMTR2 across cancer types

Previously, our pan-cancer analysis of more than 50 methyltransferases identified the 2'-O-methyltransferase FTSJ3 as a potential promoter of breast cancer progression [22]. In human cells, two Ftsj-domain-containing methyltransferases, CMTR1 and CMTR2, specifically target the mRNA cap [2, 3, 5–7]. However, our understanding of the expression patterns and biological roles of CMTR1 and CMTR2 in human cancers remains limited.

Comparing differentially expressed genes between tumor and normal samples helps to infer cancer driver genes and/or potential therapeutic targets. To determine the expression patterns of CMTR1 and CMTR2 in cancer, we analyzed their expression changes in cancerous tissues relative to normal tissues in the TCGA and CPTAC datasets. We selected tumor types with at least ten normal tissue samples available for comparison. In 15 tumor types with more than ten normal sample controls from the TCGA dataset, we found that *CMTR1* exhibited significantly ($p < 0.05$) increased RNA levels in five TCGA cancer types compared to normal adjacent tissues (NATs): breast (BRCA), bladder (BLCA), colorectal (COADREAD), head and neck (HNSC), and liver (LIHC) cancers (Fig. 1A). Conversely, *CMTR2* showed significantly decreased RNA levels in nine tumor types: BRCA, HNSC, LIHC, kidney clear cell (KIRC), kidney papillary (KIRP), lung adenocarcinoma (LUAD), lung squamous cell carcinoma (LUSC), prostate adenocarcinoma (PRAD), and endometrial carcinoma (UCEC) (Supplementary Fig. 1A & Supplementary Table 1).

The recent availability of proteomic profiles across a broad range of cancers from CPTAC projects has provided an unprecedented opportunity to investigate proteomic changes of CMTRs in cancers relative to normal tissues [48]. We analyzed protein expression differences

between tumors and NATs using CPTAC proteomics data for eight tumor types, each with at least ten NAT samples available. Our analysis revealed that CMTR1 protein was significantly upregulated in five tumor types compared to their respective NAT samples: colon (COAD), HNSC, LUAD, LUSC, and ovarian (OV) (Fig. 1B). Interestingly, we found that CMTR2 protein was significantly upregulated in several tumor types, including HNSC, KIRC, LUAD, and LUSC (Supplementary Fig. 1B & Supplementary Table 1). This upregulation occurred even in cases where CMTR2 mRNA levels were downregulated, such as in HNSC or LUSC, compared to NATs (Supplementary Fig. 1B). These results suggest an additional layer of regulation for CMTR2 protein expression, independent of mRNA expression, in certain tumor types.

Given that phosphorylation is a key process in regulating protein activity, we also analyzed CPTAC phosphoproteomics data to compare changes in CMTR1 phosphorylation between tumor and normal samples [49]. Based on the PhosphoSitePlus database, we found that CMTR1 phosphorylation sites are enriched in the N-terminal region of the protein, while CMTR2 lacks this phosphorylation-enriched region (Supplementary Fig. 2A) [50]. Additionally, phosphorylation sites of CMTR2 were barely detected in the CPTAC samples. Therefore, we focused on CMTR1 phosphorylation sites and levels in CPTAC samples. Three phosphorylation sites — S51, S53, and S66 — were detected in at least five of eight CPTAC tumor types (with at least ten samples in both tumor and normal groups), allowing for comprehensive analysis. Comparing phosphorylation levels between CPTAC tumor and normal samples, we found that phosphorylation levels of S51 and S53 were significantly upregulated in four CPTAC tumor types (Supplementary Fig. 2B, Supplementary Table 2). After normalizing phosphorylation levels to CMTR1 protein abundance we observed similar results, with S53 phosphorylation levels upregulated in five CPTAC tumor types (Fig. 1C) [38]. We also investigated whether CMTR1 acetylation differed in expression between CPTAC tumor and normal samples, finding that K14 and K123 acetylation levels were both upregulated in LUAD and LUSC (Supplementary Fig. 2B, Supplementary Table 2). Given that these phosphorylation and acetylation sites of CMTR1, including K14 in the nuclear localization sequence (NLS), S51 and S53 in the P-patch, and K123 in the G-patch region, are located within functional domains or motifs, these modifications may modulate CMTR1 localization, protein-protein interactions, and activation in certain tumor types.

Our analysis of CMTR1 data revealed an unexpected reduction in median RNA levels in all TCGA UCEC samples, contrasting with its expression patterns in other

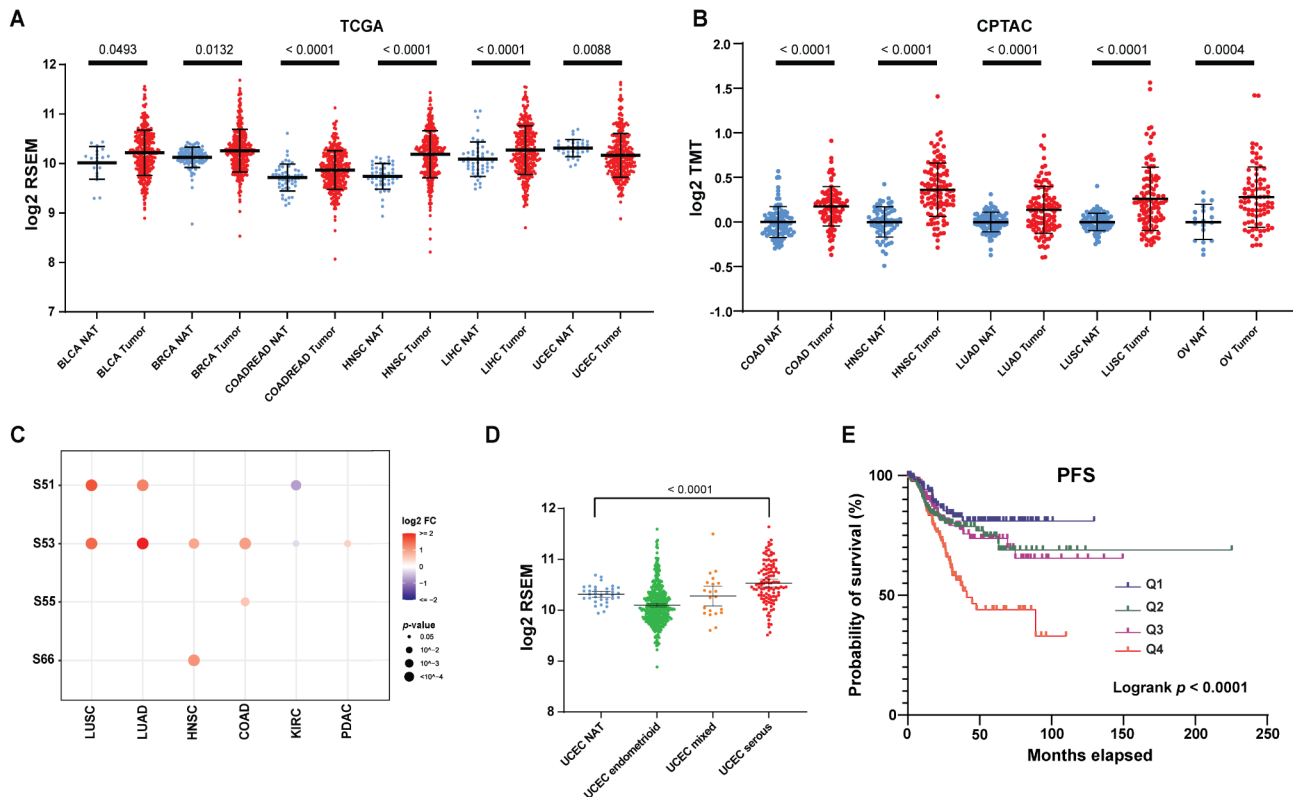


Fig. 1 CMTR1 expression, phosphorylation, and prognostic value across multiple cancer types **(A)** Dot plots of *CMTR1* mRNA expression (\log_2 RSEM) in normal and tumor samples from six TCGA cancer types. **(B)** Dot plots of *CMTR1* protein abundance (\log_2 TMT) in normal and tumor samples from five CPTAC cancer types. Blue dots represent normal adjacent tissue (NAT) samples, whereas red dots represent tumor samples. Each data point represents an individual patient sample. The p -value from a Mann-Whitney U test comparing tumor and NAT samples for each cancer type is displayed. Error bars indicate standard deviation of mRNA or protein expression levels across patients. **(C)** Normalized phosphorylation levels of *CMTR1* residues S51, S53, S55, and S66 relative to total *CMTR1* protein abundance in normal and tumor samples from six CPTAC cancer types. The heatmap displays \log_2 FC (fold-change) for cancer types with at least 10 samples in both tumor and NAT groups. The color gradient from purple to red represents the degree of \log_2 FC between tumor and normal samples. Dot size indicates statistical significance. Only data points with \log_2 FC $>|0.2|$ and p -value < 0.05 are shown. **(D)** mRNA expression levels of *CMTR1* in TCGA UCEC by histological subtypes. *CMTR1* expression is significantly higher in the serous subtype of UCEC compared to NAT samples, while it is lower in the endometrioid subtype compared to NAT samples. **(E)** Kaplan-Meier progression-free survival curves of TCGA UCEC patients ($n = 530$) stratified into quartiles (Q1, Q2, Q3 and Q4) by *CMTR1* expression. The highest expression group (Q4) is shown with a red line

tumor types (Fig. 1A). To further investigate this finding, we stratified UCEC tumors by histological subtype (endometrioid, serous, and mixed) [51–53]. This analysis showed that *CMTR1* expression is either decreased (at the RNA level) or unchanged (at the protein level) in UCEC's endometrioid subtype (Fig. 1D, Supplementary Fig. 3A). Conversely, UCEC's serous subtype, which is more aggressive than other subtypes, exhibited increased *CMTR1* expression at both RNA and protein levels (Fig. 1D, Supplementary Fig. 3A). Importantly, we found that increased *CMTR1* expression correlates with reduced progression-free and overall survival in TCGA UCEC tumor samples (Fig. 1E, Supplementary Fig. 3B). This effect appears to be largely driven by the increased expression in serous subtype tumors, which are known to have poor prognoses in UCEC [54]. Furthermore, when grouping *CMTR1* protein expression in CPTAC data by molecular subtype, we also observed increased

expression in copy number variation (CNV)-high tumors compared to both normal tissue and other UCEC molecular subtypes (Supplementary Fig. 3C). The CNV-high molecular subtype is mainly comprised of tumors with serous histology [53].

In conclusion, our analysis revealed that *CMTR1* undergoes alterations at the RNA, protein, and phosphorylation levels across multiple cancer types in the TCGA and/or CPTAC datasets.

***In vitro* and *in vivo* evidence for *CMTR1*'s tumor-promoting function**

To investigate the biological importance of *CMTR1* and *CMTR2* in various tumors, we analyzed genome-wide CRISPR screen data (DepMap 24Q2) from more than 1,000 tumor cell lines [39, 55]. *CMTR1* exhibited significantly lower cancer dependency scores compared to *CMTR2*, with mean scores of -0.79 and -0.08 ,

respectively ($p < 0.0001$). Lower scores indicate greater criticality for tumor cell growth and survival. Notably, 19.3% of cancer cell lines showed CMTR1 scores at or below -1 (the average score of critical cell survival genes), whereas only 0.09% of cell lines exhibited such scores for CMTR2 (Supplementary Fig. 4A). To further evaluate CMTR1's role in cancer cells, we employed CRISPR gene editing to knockout *Cmtr1* in the 4T1 mouse cancer cell line. We selected the 4T1 line due to its molecular similarity to human basal-like breast cancer, which also shows relatively high CMTR1 expression in CPTAC breast cancers (Supplementary Fig. 4B). In addition, our previous study of more than 50 RNA methyltransferases in TCGA breast cancers revealed that mRNA levels of *CMTR1*, but not *CMTR2*, are significantly higher in the basal-like subtype compared to the ER (estrogen receptor) - positive luminal subtype [22]. Analysis of *CMTR1* expression levels in breast cancer cell lines from the Cancer Cell Line Encyclopedia (CCLE) also revealed elevated expression in basal-like cell lines (Supplementary Fig. 5A). Western blotting assay of CMTR1 also revealed that protein expression of CMTR1 was higher in a subset of basal-like breast cancer lines (Supplementary Fig. 5B).

Next, CRISPR-mediated editing of *Cmtr1* in 4T1 cells was confirmed by DNA sequencing, and *Cmtr1* depletion

was validated by Western blot assay (Fig. 2A). *Cmtr1* depletion dramatically inhibited 4T1 cell growth compared to negative control cells (Fig. 2B). Clonal growth efficiency in soft agar is a measure of the ability of cancer cells to form colonies in a semi-solid medium, which is considered a hallmark of tumorigenicity [56]. We found that *Cmtr1* KO significantly reduced 4T1 anchorage-independent growth in soft agar (Fig. 2C). Invasion assays showed that *Cmtr1* KO significantly inhibited the invasive capacity of 4T1 cells (Fig. 2D, Supplementary Fig. 6). To corroborate these findings in human cancer cells, we used siRNA to knockdown CMTR1 in MDA-MB-436 human basal-like breast cancer cells. qRT-PCR and western blot assays revealed that siRNA significantly decreased the expression of CMTR1 at both mRNA and protein levels in MDA-MB-436 cells (Fig. 2E). Consistent with our observations in 4T1 cells, CMTR1 knockdown in MDA-MB-436 cells also inhibited growth in vitro (Fig. 2F).

To assess the in vivo relevance of our findings, we injected 4T1 *Cmtr1*-KO cells into mice. *Cmtr1* depletion significantly inhibited tumor growth in vivo (Fig. 2G). In summary, our findings indicate that CMTR1 may play a role in promoting tumor growth in the experimental models used in this study.

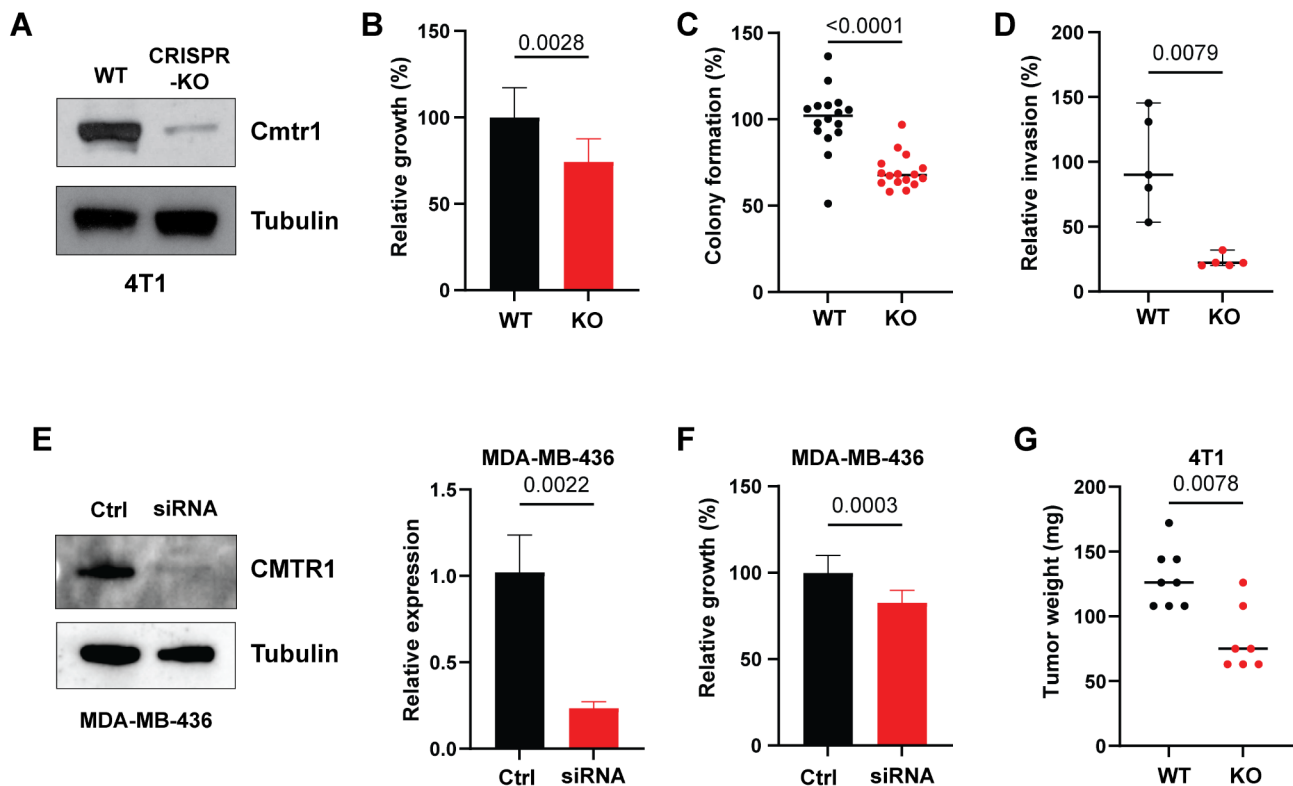


Fig. 2 CMTR1 reduces tumor growth and invasion in vitro and in vivo. (A) Immunoblot showing the expression of *Cmtr1* in the *Cmtr1*-knockout (KO) 4T1 cells. (B) in vitro growth, (C) colony formation in soft agar, and (D) invasion in *Cmtr1*-KO and control 4T1 cells. (E) Knockdown of CMTR1 in human basal-like breast cancer MDA-MB-436 cells with the siRNA was confirmed by qRT-PCR and western blot assays. (F) Bar graph shows relative cell growth after knocking down CMTR1 in MDA-MB-436 cells. (G) Tumor weight of in vivo 4T1 tumors with or without *Cmtr1* knockout. Error bars: SD (standard deviation)

CMTR1 depletion leads to downregulation of ribosomal protein genes across cancer cell lines

We next investigated the transcriptomic effects of *Cmtr1* depletion using our 4T1 CRISPR KO model. RNA-Seq analysis revealed 196 genes with reduced expression and 21 genes with increased expression in *Cmtr1*-KO cells, using a stringent cut-off for our RNA-seq analysis [adjusted p -value (q -value) < 0.05] (Fig. 3A). Pathway analyses using Enrichr showed that downregulated genes were significantly associated with two pathways: ribosome ($p = 5.20E-74$, $q = 2.34E-72$) and oxidative phosphorylation ($p = 0.0019$, $q = 0.04577$) [42, 43]. Notably, 57 out of 196 downregulated genes were ribosomal pathway members (Fig. 3A, Supplementary Table 3). No significant pathways were identified for upregulated genes. To validate these findings, we also analyzed published RNA-Seq datasets from the lung cancer cell line A549 with or without CMTR1 depletion, previously used to identify host dependency factors for influenza A virus infection [18]. In A549 cells, with and without IFN treatment (A549NT and A549IFN respectively), we confirmed that the top downregulated genes were significantly enriched in ribosome pathways, primarily ribosomal proteins ($p = 2.82E-55$, $q = 8.73E-53$ and $p = 6.59E-46$, $q = 2.07E-43$, respectively) (Supplementary Fig. 7A-B, Supplementary Tables 4–5). Intersecting all three datasets (4T1, A549NT, and A549 IFN) revealed 64 genes commonly downregulated, while only one gene, *LARP4* (La ribonucleoprotein 4), was commonly upregulated (Fig. 3B, Supplementary Table 6A, Supplementary Fig. 7C). Again, pathway analysis of the common downregulated gene set showed 53 of 64 genes were ribosomal protein genes (Fig. 3B, Supplementary Table 6B). We confirmed the downregulation of multiple ribosomal protein genes (e.g., *RPS10*, *RPS14*, and *RPL13A*) upon CMTR1 loss via qRT-PCR in both our 4T1 *Cmtr1*-KO model and an MDA-MB-231 CMTR1 siRNA model (Fig. 3C, Supplementary Fig. 8).

In summary, our data, together with previously published findings, indicate that ribosomal protein genes are among the primary targets regulated by CMTR1 in some cancer types.

Enrichment of TOP elements in CMTR1-regulated genes

Expression of ribosomal proteins and other factors required for protein synthesis is crucial for cellular function. The 5' Terminal Oligopyrimidine (TOP) motif, characterized by a cytosine as the first nucleotide followed by 4–15 pyrimidines (C/U), is found in transcripts encoding all human ribosomal proteins, as well as various initiation factors, elongation factors, and other proteins essential for translation [57]. Given that ribosomal protein genes were among the most significantly modulated transcripts following CMTR1 depletion in cancer cells,

we hypothesized that CMTR1-regulated transcripts are enriched for 5' TOP elements.

To test this hypothesis, we utilized a recently developed TOP score metric tool to quantify TOP elements in transcripts [58]. We calculated TOP scores from our 4T1 transcription profiles following *Cmtr1* depletion, as well as the common gene set. Our analysis revealed that genes downregulated after *Cmtr1* depletion were significantly enriched for TOP elements, exhibiting dramatically increased TOP scores compared to other genes (Fig. 4A). These data suggest that CMTR1 deficiency predominantly affects a set of 5'-TOP motif-containing mRNAs, including those encoding ribosomal proteins and other components of the translational machinery in cancer cells. However, the detailed molecular mechanism underlying this regulation requires further investigation.

Downregulation of snorna host genes and snornas following CMTR1 depletion

SnoRNAs and their host genes play important roles in several biological processes, including rRNA modification and ribosome biosynthesis [59]. In the human genome, most snoRNA genes are located within the introns of other 'host' genes, which can be either protein-coding (many of which are ribosomal protein genes) or non-coding. Interestingly, our integrated RNA-seq analysis revealed that CMTR1 depletion in cancer cells led to the downregulation of five snoRNA non-coding host genes (*SNHG1*, *SNHG8*, *SNHG12*, *GASS5*, *ZFAS1*) and 21 snoRNA protein-coding host genes (e.g., *RPS11*, *RPL39*) (Supplementary Table 6A). To validate these findings, we performed qRT-PCR assays to measure the expression of snoRNA host genes in our CMTR1-depleted breast cancer cells. Our results confirmed that CMTR1 depletion induced the downregulation of these host genes, including *SNHG8*, *GASS5*, and *ZFAS1* (Figs. 3C and 4B). Of particular interest, *ZFAS1*, which encodes three C/D box SNORD12 family members (*SNORD12*, *SNORD12B*, and *SNORD12C*), is significantly overexpressed in various human cancers [60–62]. Our qRT-PCR assays further showed that two snoRNAs, *Snord12b* and *Snord12c*, were significantly downregulated in our *Cmtr1*-KO 4T1 cells compared to controls (Fig. 4B). These data suggest that CMTR1 overexpression in cancer cells likely supports cell growth and cancer phenotypes through multiple mechanisms, including the regulation of both protein-coding and non-coding gene expression.

In silico and in vitro screening for novel CMTR1 inhibitors

To further investigate the potential of CMTR1 as a therapeutic target in cancer, we sought to identify novel inhibitors of this enzyme using a combination of in silico and in vitro approaches. The crystal structure of the CMTR1 enzymatic domain in complex with m7G RNA has been

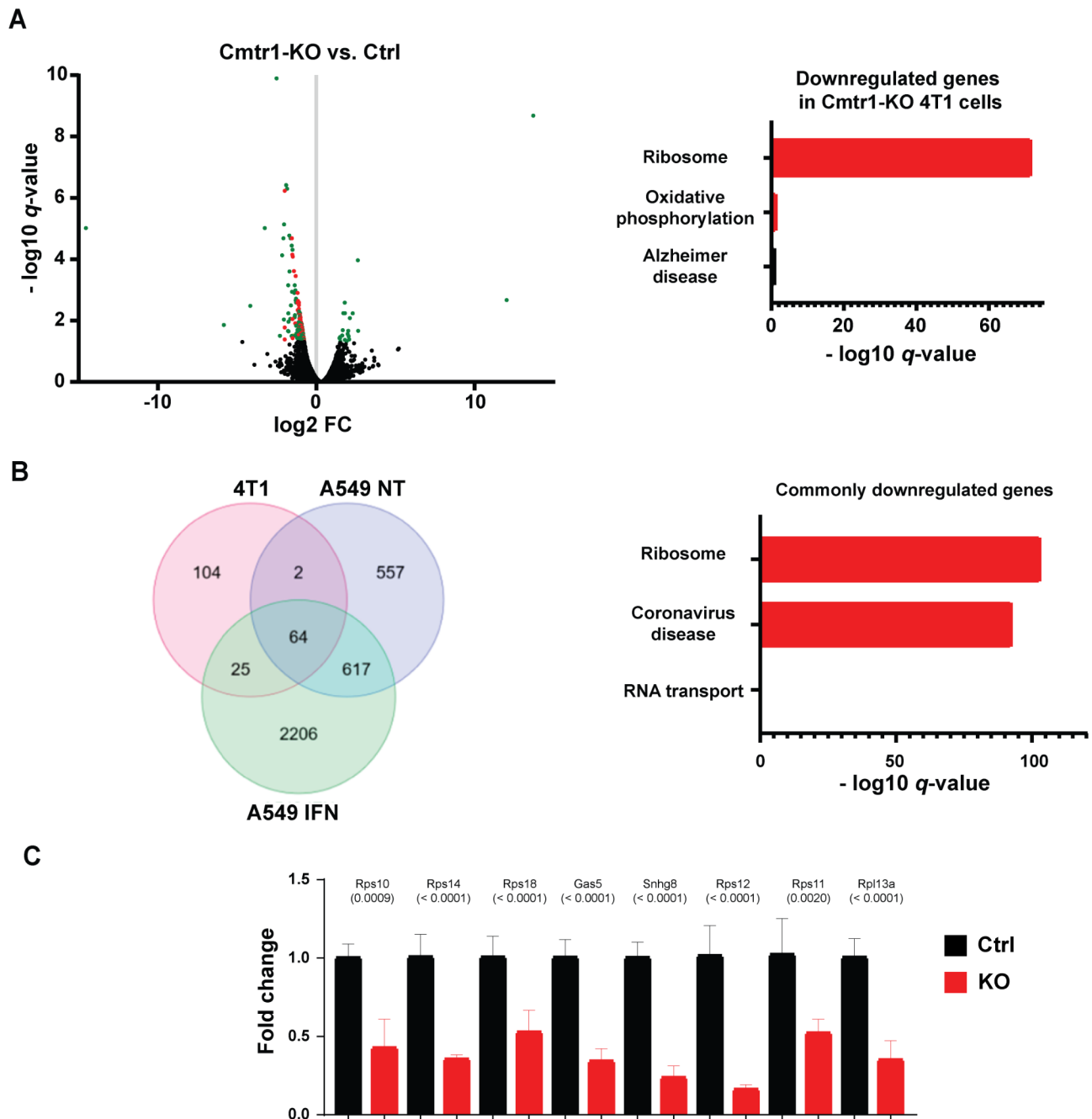


Fig. 3 CMTR1 loss reduces ribosomal protein gene expression in cancer cell lines. **(A)** Volcano plot of differentially expressed genes in 4T1 cells after Cmtr1 knockout (left), with pathway analysis of downregulated genes (right). Each dot represents a gene. Green dots indicate significantly ($q < 0.05$) up- and down-regulated genes in Cmtr1 knockout 4T1 cells, while red dots highlight significantly down-regulated ribosomal protein genes or SNHGs. In the right panel, pathway analyses using Enrichr was performed on the significantly down-regulated genes in Cmtr1 knockout 4T1 cells. For the pathway analysis, red is significant, and the longer the bar the more significant the pathway. **(B)** Intersection of genes downregulated upon CMTR1 knockout (KO) in three cell models (4T1, A549 untreated, and A549 IFN-treated; left), and pathway analysis of commonly downregulated genes (right). In the right panel, pathway analyses using Enrichr was performed on the common significantly down-regulated genes in CMTR1 knockout cells. For the pathway analysis, red is significant, and the longer the bar the more significant the pathway. **(C)** Relative expression levels of eight ribosomal protein genes or non-coding SNHGs measured by qRT-PCR in 4T1 cells after Cmtr1 knockout. p -values for each gene, determined by Welch's t-test, are displayed. Ctrl: Control; KO: Cmtr1 knockout. Error bars: SD

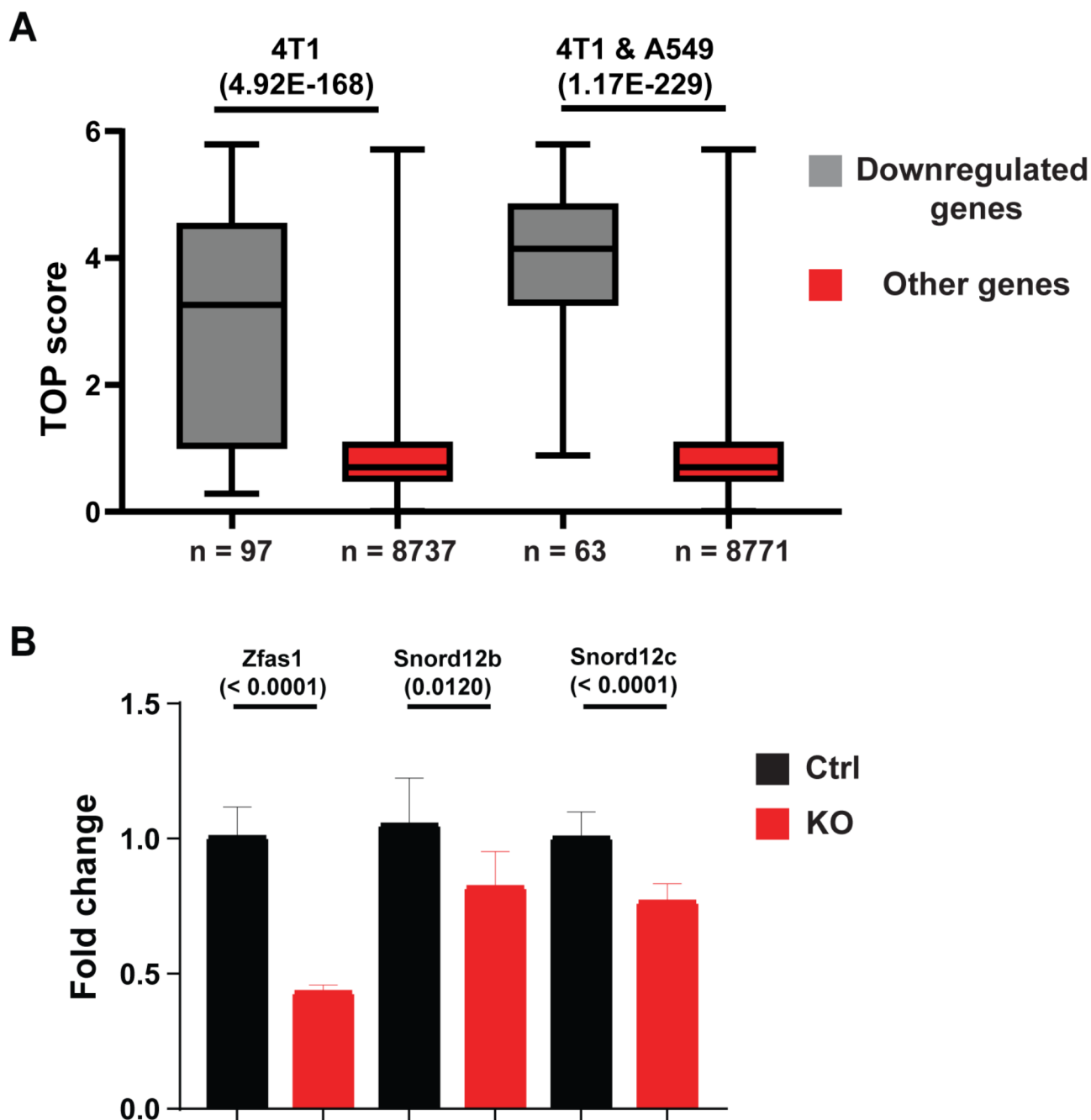


Fig. 4 CMTR1 inhibition affects 5'TOP mRNAs and snoRNA expression in cancer cells. **(A)** Boxplots show the patterns of 5'TOP scores for downregulated genes in 4T1 Cmtr1-KO cells or the common downregulated gene set as shown in Fig. 3B compared to all other genes. TOP scores for each gene were retrieved from a published dataset that calculated features of TOP sequences [58]. The differences between downregulated genes in the Cmtr1-KO 4T1 model and the three models (4T1, A549NT, and A549IFN) compared with all other genes were calculated using Student's t-test. **(B)** Relative expression levels of the snoRNA host gene *Zfas1* and its associated snoRNAs (*Snord12b* and *Snord12c*) measured by qRT-PCR in 4T1 cells after *Cmtr1* knockout. *p*-values for each RNA, determined by Welch's t-test, are displayed. Ctrl: Control; KO: Cmtr1 knockout. Error bars: SD

experimentally solved, and critical residues, such as lysine (K) 203, have been demonstrated to be structurally and functionally important for CMTR1 activity (Fig. 5A) [12]. Accordingly, we used UCSF-Chimera and Autodock software to optimize the 1.9-Å crystal structure of CMTR1 enzymatic domain (PDB: 4N49) for virtual screening

[63–66]. Three NCI compound sets, the Diversity set (derived from ~140,000 compounds), Mechanistic set (derived from 37,836 compounds), and Natural Products set (selected from ~140,000 compounds) were screened (Fig. 5B) [63]. From this initial screen, 18 compounds were selected for validation using BLI assays (Fig. 5C).

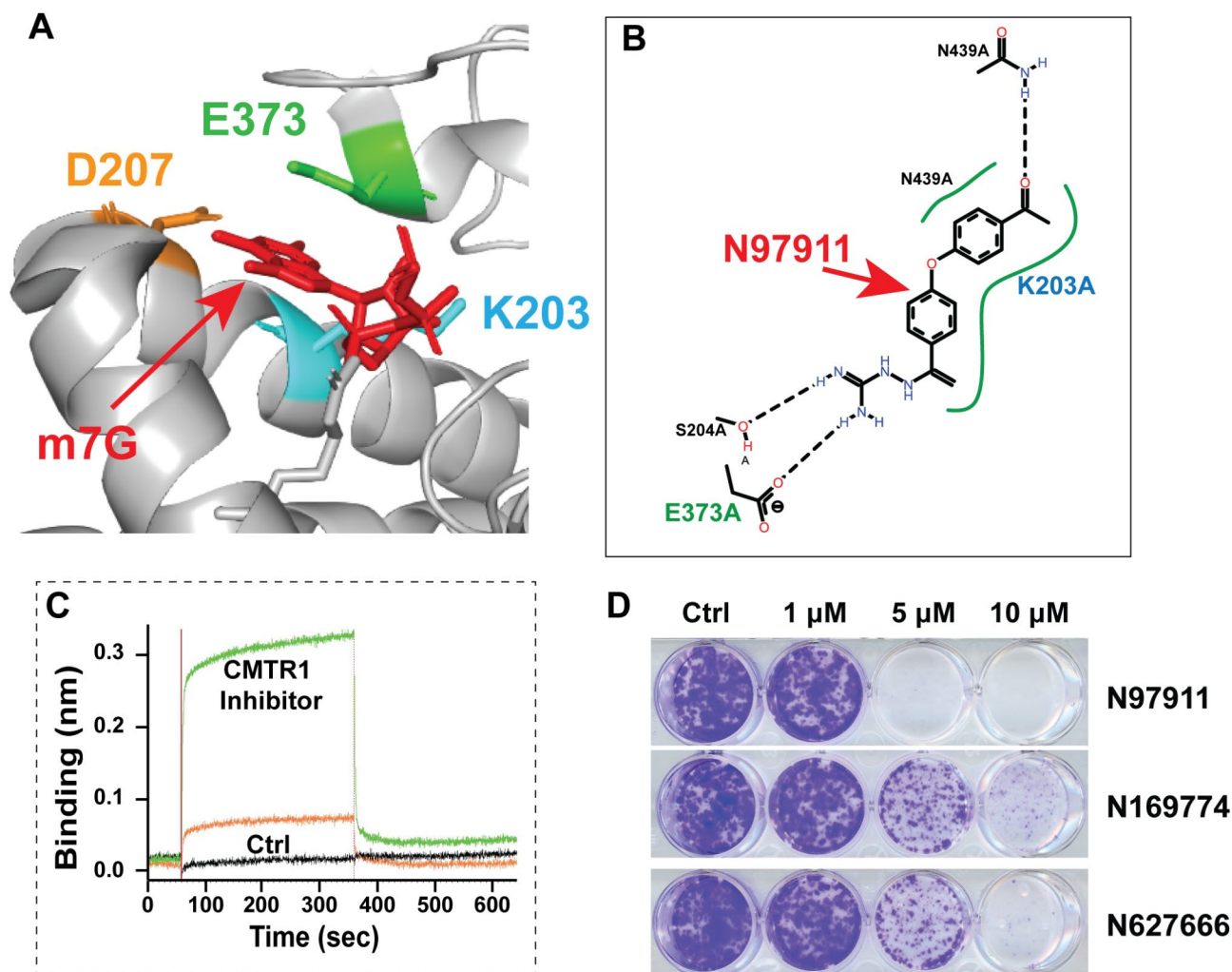


Fig. 5 Identification of novel CMTR1 inhibitors: N97911, N169774 and N627666. **(A)** Ribbon diagram, generated with PyMOL, showing the CMTR1 enzymatic domain in complex with m7G RNA (PDB: 4N49). Three key residues, K203, D207, and E373, along with m7G RNA, are shown and labeled in color. **(B)** Two-dimensional (2D) representation of the predicted N97911–CMTR1 binding mode, generated using PoseView. Dashed lines indicate hydrogen bonds and green colored lines indicate pi-pi interactions. **(C)** Association/dissociation binding curves (BLI assay) of one CMTR1 candidate inhibitor (N169774) to the immobilized CMTR1 protein. The green line represents a 20 μM concentration, the orange line represents a 5 μM concentration of the N169774 compound, and the black line represents the vehicle (DMSO) control. **(D)** Representative images of clonogenic survival in 4T1 cells after treatment with three CMTR1 candidate inhibitors

Our analysis identified three lead compounds—N97911, N169774, and N627666—that demonstrated potential to block CMTR1-m7G RNA binding. Further examination of their binding modes to the CMTR1 enzymatic domain revealed that all three compounds exhibit hydrophobic interactions and/or pi-pi interactions with key residue(s) of the m7G RNA pocket (Fig. 5B). Notably, data from the NCI Developmental Therapeutics Program indicated that N97911 displayed substantial growth inhibition activity against a set of NCI-60 cancer lines, including ovarian cancer lines (data not shown). We subsequently confirmed that these CMTR1 candidate compounds, particularly N97911, inhibited 4T1 cancer cell growth and survival in vitro (Fig. 5D). While further studies are necessary, our identified CMTR1 inhibitor candidates

provide starting points to identify more potent inhibitors and suggest the therapeutic potential of targeting CMTR1 in certain cancer types.

Discussion

In this study, we employed a multi-omics approach, combining transcriptomics, proteomics, and functional genomics to elucidate the clinical and biological significance of cap methyltransferases, focusing primarily on CMTR1, in various human cancers. Our analysis revealed differential expression of CMTR1 and CMTR2 across cancer types, with CMTR1, but not CMTR2, showing upregulation at both mRNA and protein levels in several cancer types examined. Functionally, CMTR1 depletion significantly inhibited tumor growth both in vitro and in

vivo. At the molecular level, we found that CMTR1 regulates the expression of ribosomal protein genes and other transcripts with 5' TOP motifs. Additionally, CMTR1 affects the expression of snoRNA host genes and snoRNAs, suggesting a broader role in RNA metabolism. Finally, we explored the potential of CMTR1 as a therapeutic target by identifying candidate inhibitors. While further studies are necessary, these CMTR1 inhibitor candidates provide promising starting points for developing more potent inhibitors and highlight the therapeutic potential of targeting CMTR1 in various cancers.

CMTR1 was originally identified in 2008 as an interferon-stimulated gene (ISG), initially designated as *ISG95*, whose expression increases in response to interferon treatment and viral infection [16]. This early study also revealed that CMTR1 interacts with the CTD of RNA polymerase II, suggesting CMTR1's potential role in regulating gene expression and its involvement in mRNA processing events. Subsequently, Bélanger et al. biochemically characterized CMTR1 and revealed that it functions as the 2'-O-ribose methyltransferase responsible for cap1 formation in higher eukaryotic cells [14]. In contrast, its homolog CMTR2, methylates the 2'-O-ribose of the second transcribed nucleotide, forming cap2 structures [13]. Structurally, in addition to the Ftsj methyltransferase domain, CMTR1 contains multiple non-enzymatic domains or motifs, including an N-terminal NLS, a G-patch domain, a C-terminal inactive cap guanylyltransferase-like (GTase-like) domain, and a WW domain (Supplementary Fig. 2A) [4, 14–16, 19]. A very recent study identified that CMTR1 also contains a highly phosphorylated 'P-patch' motif, which is targeted by the kinase CK2 (casein kinase II) [19]. In contrast, CMTR2 contains only the enzymatic Ftsj methyltransferase domain and a catalytically inactive methyltransferase domain [12].

Previous studies revealed that the non-enzymatic domains of CMTR1 interact with various proteins, influencing both the enzymatic activity of CMTR1 and transcriptional regulation [14–16]. Early studies revealed that the WW domain of CMTR1 interacts with the Ser-5 phosphorylated CTD of RNA Pol II [15, 16]. Two recent structural studies of human co-transcriptional capping demonstrated that the C-terminal GTase-like domain of CMTR1 also directly interacts with Pol II, likely playing a role in the recruitment of CMTR1 to the Pol II surface [67, 68]. Furthermore, these studies revealed that CMTR1 directly binds to the paused elongation complex, which includes DRB sensitivity-inducing factor (DSIF) and negative elongation factor (NELF) [67, 68]. These structural studies revealed the co-existence of CMTR1 with pausing factors, suggesting an intricate relationship between 5' end capping modifications and the transcriptional pausing of Pol II.

CMTR1 also contains a G-patch, a glycine-rich 50-residue motif found in approximately 20 human proteins [15]. Notably, CMTR1 is the only human G-patch protein that possesses a catalytic domain [69]. Among these G-patch proteins, more than ten, including CMTR1, have been identified to interact with the OB-fold (oligonucleotide/oligosaccharide-binding fold) of the RNA helicase DHX15 (DEAH-Box Helicase 15), with most of these interactions enhancing DHX15's enzymatic activity [69]. Regarding the CMTR1-DHX15 interaction, Inesta-Vaquera et al. suggest that CMTR1-DHX15 interactions reduce the methyltransferase activity of CMTR1 while increasing the helicase activity of DHX15 [15]. In contrast, Toczydlowska-Socha et al. propose that DHX15 facilitates CMTR1's methyltransferase activity on mRNAs with highly structured 5' ends, while CMTR1 enhances DHX15's ATPase activity, though not its helicase activity. DHX15 is a multifunctional RNA helicase involved in RNA splicing, ribosome biogenesis, viral RNA sensing, and other cellular processes [70]. Analysis of CPTAC cancer datasets revealed that the DHX15 protein is highly expressed in cancer samples compared to normal tissues and is significantly positively correlated with CMTR1 protein expression (Supplementary Fig. 9). These protein correlation data provide additional evidence of the positive interconnection and interplay between CMTR1 and DHX15. However, further mechanistic studies are needed to fully understand how these proteins work together to promote cancer progression.

In this study, we observed significantly upregulated phosphorylation of CMTR1 at S51 and S53 in multiple tumor types (Supplementary Fig. 2B, Supplementary Table 2). These sites are located within the P-patch motif of the CMTR1 protein. Recently, Lukoszek et al. demonstrated that phosphorylation of the P-patch by CK2 kinase enhances CMTR1's interaction with the CTD of Pol II, thereby promoting RNA cap formation and cell proliferation without significantly affecting its methyltransferase activity [19]. To identify additional kinases that may target S51 and S53 phosphorylation of CMTR1, we performed an in silico kinome-wide analysis using the Kinase Prediction tool at PhosphoSitePlus [71, 72]. Our in silico analysis supports CK2 as a primary kinase targeting S53 and identifies potential kinases for S51, including SMG1 (SMG1 nonsense mediated mRNA decay associated PI3K related kinase) and BIKE (BMP2 inducible kinase), as well as MEK1 (MAP kinase/ ERK kinase 1) and CDC7 (cell division cycle 7) for S53 of CMTR1 (Supplementary Table 7). Further in vitro and in vivo assays are needed to validate whether these candidate kinases phosphorylate CMTR1 and to elucidate how these kinases regulate CMTR1 function in both physiological and pathological contexts.

Recent studies using knockout mice for *Cmtr1* and *Cmtr2* revealed that the loss of either *Cmtr1* or *Cmtr2* results in lethality; however, the sets of misregulated transcripts do not overlap [73, 74]. Using *Cmtr1*-conditional knockout mice, Lee et al. found that *Cmtr1*-catalyzed 2'-O-ribose methylation controls neuronal development by regulating *Camk2α* (Calcium/Calmodulin Dependent Protein Kinase II Alpha) expression [75]. Studies also demonstrated that CMTR1 plays an important role in the differentiation of embryonic stem cells by promoting the expression of ribosomal proteins and histone genes [17, 76]. Notably, our RNA-seq analysis in various cancer models also revealed that CMTR1 regulates the expression of ribosomal protein genes but not histone genes. These findings suggest that ribosomal protein genes are commonly regulated downstream of CMTR1, possibly via CMTR1 recognition of transcripts bearing 5' TOP motifs. Consequently, one mechanism through which CMTR1 supports cancer cell growth may involve increasing ribosomal protein gene expression, thereby promoting ribosome biogenesis.

Prior to our study, research on CMTR1 in cancer was limited but provided initial insights into its potential roles. In 2018, Du et al. reported a *CMTR1-ALK* fusion in non-small-cell lung cancer that did not respond to the ALK inhibitor crizotinib, suggesting a possible role for CMTR1 in drug resistance [33]. More recently, You et al. demonstrated that CMTR1 promotes colorectal cancer cell growth and immune evasion by transcriptionally regulating STAT3 [34]. They showed that CMTR1 knockdown reduced colon cancer cell proliferation and tumor growth in vivo, while also enhancing the efficacy of anti-PD-1 therapy [34]. Previous studies have also revealed that CMTR1 knockdown inhibits in vitro cell proliferation of human MCF7 and HCC1806 breast cancer cell lines [15]. In this study, we also revealed that increased CMTR1 expression correlates with reduced progression-free and overall survival in TCGA UCEC tumor samples. Furthermore, by querying the TCGA database, we identified a significant association between higher CMTR1 expression and worse clinical outcomes in several other cancer types, including KIRC, PRAD, sarcoma (SARC), and acute myeloid leukemia (LAML), as shown by the survival curves of CMTR1 in KIRC and LAML. (Supplemental Fig. 10) [77, 78]. Together, our work advances our understanding of CMTR1 in cancer, as well as a set of common genes (especially ribosomal) regulated by CMTR1 across tumor types.

Conclusion

Our comprehensive study establishes CMTR1 as a critical player in cancer biology, demonstrating its widespread upregulation in some tumor types and impacts on cell growth, ribosomal protein gene expression, and

snoRNA regulation. Our discovery of a potential CMTR1 inhibitor opens promising avenues for therapeutic intervention. While these findings advance our understanding of CMTR1 in cancer, they also highlight the need for further research to fully elucidate the protein-level effects of CMTR1 depletion, its impact on ribosomal function, and its interplay with other cap methyltransferases. As we continue to unravel the complexities of CMTR1's role in cancer, this enzyme emerges as a promising target for novel therapies in cancer and other diseases, such as viral infections.

Abbreviations

CMTR1	Cap methyltransferase 1
CMTR2	Cap methyltransferase 2
TCGA	The cancer genome atlas
CPTAC	Clinical proteomic tumor analysis consortium
CRISPR	Clustered regularly interspaced short palindromic repeats
TOP	Terminal oligopyrimidine
RNA Pol II	RNA polymerase II
RNGTT	RNA guanylyltransferase and triphosphatase
RNMT	RNA guanine-7 methyltransferase
CTD	C-terminal domain
PCIF1	Phosphorylated CTD interacting factor 1
WT	Wild-type
KO	Knockout
SpCas9	Streptococcus pyogenes Cas9
RNP	Ribonucleoprotein
PCR	Polymerase chain reaction
siRNA	small interfering RNA
esiRNA	Endoribonuclease-prepared siRNA
KEGG	Kyoto encyclopedia of genes and genomes
RT	Reverse transcription
PUM1	Pumilio RNA binding family member 1
Gapdh	Glyceraldehyde-3-phosphate dehydrogenase
PDB	Protein data bank
BLI	Bio-layer interferometry
FTSJ3	FtsJ RNA 2'-O-methyltransferase 3
BRCA	Breast invasive carcinoma
BLCA	Bladder urothelial carcinoma
COAD	Colon adenocarcinoma
ESCA	Esophageal carcinoma
HNSC	Head and neck squamous cell carcinoma
KIRC	Kidney renal clear cell carcinoma
KIRP	Kidney renal papillary cell carcinoma
LIHC	Liver hepatocellular carcinoma
LUAD	Lung adenocarcinoma
LUSC	Lung squamous cell carcinoma
OV	Ovarian serous cystadenocarcinoma
READ	Rectum adenocarcinoma
PRAD	Prostate adenocarcinoma
UCEC	Uterine corpus endometrial carcinoma
SARC	Sarcoma
LAML	Acute myeloid leukemia
CNV	Copy number variation
qRT-PCR	Quantitative reverse transcription polymerase chain reaction
IFN	Interferon
LARP4	La ribonucleoprotein 4
SNHG	Small nucleolar RNA host gene
GAS5	Growth arrest specific 5
ZFAS1	ZNF1(zinc finger NFX1-type containing 1) antisense RNA 1
snoRNA	Small nucleolar RNA
SNORD	Small nucleolar RNA, C/D box
m7G	N7-methylguanosine
ISG	Interferon-stimulated gene
GTase-like	Guanylyltransferase-like
CK2	Casein kinase II
DSIF	DRB sensitivity-inducing factor

NELF	Negative elongation factor
OB-fold	Oligonucleotide/oligosaccharide-binding fold
DHX15	DEAH-box helicase 15
Camk2a	Calcium/calmodulin dependent protein kinase II alpha
ALK	ALK receptor tyrosine kinase
STAT3	Signal transducer and activator of transcription 3
FC	Fold-change
PFS	Progression-free survival
OS	Overall survival
SMG1	SMG1 nonsense mediated mRNA decay associated PI3K related kinase
BIKE	BMP2 inducible kinase
MEK1	MAP kinase/ ERK kinase 1
CDC7	Cell division cycle 7

Supplementary Information

The online version contains supplementary material available at <https://doi.org/10.1186/s12964-025-02147-6>.

Supplementary Material 1

Acknowledgements

We thank Paul Stemmer, Lanxin Liu, Rui Wang, Juiwanna Kushner, Maksymilian Pilecki, Ivan Lopez and Morenci Manning for technical contributions.

Author contributions

I.C. conceived of the study, carried out the bioinformatic analyses, growth and colony formation assays and qPCRs, and drafted the manuscript. Y.J. and H.A. participated in model generation, PCR, western blot and functional assays. S.D. and L.P. performed the in vivo work. Z.Y. conceived, designed, funded, and participated in its design and coordination and drafted the manuscript. All authors read and approved the final manuscript.

Funding

This work was partially supported by grants from the Department of Defense (DoD) Breast Cancer Program BC201476, Elsa U. Pardee Foundation, DMC Foundation and Molecular Therapeutics Program of Karmanos Cancer Institute to Dr. Zeng-Quan Yang. The Animal Model and Therapeutics Evaluation, and Proteomics Cores were supported in part by NIH Center grant P30 CA22453 to the Barbara Ann Karmanos Cancer Institute.

Data availability

No datasets were generated or analysed during the current study.

Declarations

Ethics approval and consent to participate

Not applicable.

Consent for publication

Not applicable.

Competing interests

The authors declare no competing interests.

Received: 21 November 2024 / Accepted: 9 March 2025

Published online: 24 April 2025

References

- Avila-Bonilla RG, Macias S. The molecular language of RNA 5' ends: guardians of RNA identity and immunity. *RNA*. 2024;30(4):327–36.
- Ramanathan A, Robb GB, Chan SH. mRNA capping: biological functions and applications. *Nucleic Acids Res*. 2016;44(16):7511–26.
- Inesta-Vaquera F, Cowling VH. Regulation and function of CMTR1-dependent mRNA cap methylation. *Wiley Interdiscip Rev RNA* 2017; 8(6).
- Liang S, Almohammed R, Cowling VH. The RNA cap methyltransferases RNMT and CMTR1 co-ordinate gene expression during neural differentiation. *Biochem Soc Trans*. 2023;51(3):1131–41.
- Borden K, Culjkovic-Kraljacic B, Cowling VH. To cap it all off, again: dynamic capping and recapping of coding and non-coding RNAs to control transcript fate and biological activity. *Cell Cycle*. 2021;20(14):1347–60.
- Pelletier J, Schmeing TM, Sonenberg N. The multifaceted eukaryotic cap structure. *Wiley Interdiscip Rev RNA*. 2021;12(2):e1636.
- Cowling VH. Regulation of mRNA cap methylation. *Biochem J*. 2009;425(2):295–302.
- Yamada-Okabe T, Doi R, Shimmi O, Arisawa M, Yamada-Okabe H. Isolation and characterization of a human cDNA for mRNA 5'-capping enzyme. *Nucleic Acids Res*. 1998;26(7):1700–6.
- Bugl H, Fauman EB, Staker BL, Zheng F, Kushner SR, Saper MA, Bardwell JC, Jakob U. RNA methylation under heat shock control. *Mol Cell*. 2000;6(2):349–60.
- Zhou KI, Pecot CV, Holley CL. 2'-O-methylation (Nm) in RNA: progress, challenges, and future directions. *RNA*. 2024;30(5):570–82.
- Falnes PO. Closing in on human methylation-the versatile family of seven-beta-strand (METTL) methyltransferases. *Nucleic Acids Res*. 2024;52(19):11423–41.
- Smietanski M, Werner M, Purta E, Kaminska KH, Stepinski J, Darzynkiewicz E, Nowotny M, Bujnicki JM. Structural analysis of human 2'-O-ribose methyltransferases involved in mRNA cap structure formation. *Nat Commun*. 2014;5:3004.
- Werner M, Purta E, Kaminska KH, Cymerman IA, Campbell DA, Mitra B, Zamudio JR, Sturm NR, Jaworski J, Bujnicki JM. 2'-O-ribose methylation of cap2 in human: function and evolution in a horizontally mobile family. *Nucleic Acids Res*. 2011;39(11):4756–68.
- Belanger F, Stepinski J, Darzynkiewicz E, Pelletier J. Characterization of hMTr1, a human Cap1 2'-O-ribose methyltransferase. *J Biol Chem*. 2010;285(43):33037–44.
- Inesta-Vaquera F, Chaugule VK, Galloway A, Chandler L, Rojas-Fernandez A, Weidlich S, Peggie M, Cowling VH. DHX15 regulates CMTR1-dependent gene expression and cell proliferation. *Life Sci Alliance*. 2018;1(3):e201800092.
- Haline-Vaz T, Silva TC, Zanchin NI. The human interferon-regulated ISG95 protein interacts with RNA polymerase II and shows methyltransferase activity. *Biochem Biophys Res Commun*. 2008;372(4):719–24.
- Liang S, Silva JC, Suska O, Lukoszek R, Almohammed R, Cowling VH. CMTR1 is recruited to transcription start sites and promotes ribosomal protein and histone gene expression in embryonic stem cells. *Nucleic Acids Res*. 2022;50(5):2905–22.
- Li B, Clohisey SM, Chia BS, Wang B, Cui A, Eisenhaure T, Schweitzer LD, Hoover P, Parkinson NJ, Nachshon A, et al. Genome-wide CRISPR screen identifies host dependency factors for influenza A virus infection. *Nat Commun*. 2020;11(1):164.
- Lukoszek R, Inesta-Vaquera F, Brett NJM, Liang S, Hepburn LA, Hughes DJ, Pirillo C, Roberts EW, Cowling VH. CK2 phosphorylation of CMTR1 promotes RNA cap formation and influenza virus infection. *Cell Rep*. 2024;43(7):114405.
- Williams GD, Gokhale NS, Snider DL, Horner SM. The mRNA Cap 2'-O-Methyltransferase CMTR1 Regulates the Expression of Certain Interferon-Stimulated Genes. *mSphere* 2020;5(3).
- Li S, Mason CE. The pivotal regulatory landscape of RNA modifications. *Annu Rev Genom Hum G*. 2014;15:127–50.
- Manning M, Jiang Y, Wang R, Liu L, Rode S, Bonahoom M, Kim S, Yang ZQ. Pan-cancer analysis of RNA methyltransferases identifies FTSJ3 as a potential regulator of breast cancer progression. *Rna Biol*. 2020;17(4):474–86.
- Barbieri I, Kouzarides T. Role of RNA modifications in cancer. *Nat Rev Cancer*. 2020;20(6):303–22.
- Miano V, Codino A, Pandolfini L, Barbieri I. The non-coding epitranscriptome in cancer. *Brief Funct Genomics*. 2021;20(2):94–105.
- Yanas A, Liu KF. RNA modifications and the link to human disease. *Method Enzymol*. 2019;626:133–46.
- Campeanu IJ, Jiang Y, Liu L, Pilecki M, Najor A, Cobani E, Manning M, Zhang XM, Yang ZQ. Multi-omics integration of methyltransferase-like protein family reveals clinical outcomes and functional signatures in human cancer. *Sci Rep*. 2021;11(1):14784.
- Orsolic I, Carrier A, Esteller M. Genetic and epigenetic defects of the RNA modification machinery in cancer. *Trends Genet*. 2023;39(1):74–88.
- Primac I, Penning A, Fuks F. Cancer epitranscriptomics in a nutshell. *Curr Opin Genet Dev*. 2022;75:101924.

29. Lopez J, Blanco S. Exploring the role of ribosomal RNA modifications in cancer. *Curr Opin Genet Dev.* 2024;86:102204.
30. Huang S, Tan C, Zheng J, Huang Z, Li Z, Lv Z, Chen W, Chen M, Yuan X, Chen C, et al. Identification of RNMT as an immunotherapeutic and prognostic biomarker: from pan-cancer analysis to lung squamous cell carcinoma validation. *Immunobiology.* 2024;229(5):152836.
31. Dunn S, Lombardi O, Lukoszek R, Cowling VH. Oncogenic PIK3CA mutations increase dependency on the mRNA cap methyltransferase, RNMT, in breast cancer cells. *Open Biol.* 2019;9(4):190052.
32. Xiang B, Zhang M, Li K, Zhang Z, Liu Y, Gao M, Wang X, Xiao X, Sun Y, He C, et al. The epitranscriptional factor PCIF1 orchestrates CD8(+) T cell ferroptosis and activation to control antitumor immunity. *Nat Immunol.* 2025;26(2):252–64.
33. Du X, Shao Y, Gao H, Zhang X, Zhang H, Ban Y, Qin H, Tai Y. CMTR1-ALK: an ALK fusion in a patient with no response to ALK inhibitor Crizotinib. *Cancer Biol Ther.* 2018;19(11):962–6.
34. You AB, Yang H, Lai CP, Lei W, Yang L, Lin JL, Liu SC, Ding N, Ye F. CMTR1 promotes colorectal cancer cell growth and immune evasion by transcriptionally regulating STAT3. *Cell Death Dis.* 2023;14(4):245.
35. Bao B, Tian M, Wang X, Yang C, Qu J, Zhou S, Cheng Y, Tong Q, Zheng L. SNORA37/CMTR1/ELAVL1 feedback loop drives gastric cancer progression via facilitating CD44 alternative splicing. *J Exp Clin Cancer Res.* 2025;44(1):15.
36. Liao Y, Savage SR, Dou Y, Shi Z, Yi X, Jiang W, Lei JT, Zhang B. A proteogenomics data-driven knowledge base of human cancer. *Cell Syst.* 2023;14(9):777–e787775.
37. Vasaikar SV, Straub P, Wang J, Zhang B. LinkedOmics: analyzing multi-omics data within and across 32 cancer types. *Nucleic Acids Res.* 2018;46(D1):D956–63.
38. Wang D, Qian X, Du YN, Sanchez-Solana B, Chen K, Kanigicherla M, Jenkins LM, Luo J, Eng S, Park B, et al. cProSite: A web based interactive platform for online proteomics, phosphoproteomics, and genomics data analysis. *J Biotechnol Biomed.* 2023;6(4):573–8.
39. Tsherniak A, Vazquez F, Montgomery PG, Weir BA, Kryukov G, Cowley GS, Gill S, Harrington WF, Pantel S, Krill-Burger JM, et al. Defining a cancer dependency map. *Cell.* 2017;170(3):564–e576516.
40. Mahi NA, Najafabadi MF, Pilarczyk M, Kouril M, Medvedovic M. GREIN: an interactive web platform for Re-analyzing GEO RNA-seq data. *Sci Rep.* 2019;9(1):7580.
41. Yang ZQ, Streicher KL, Ray ME, Abrams J, Ethier SP. Multiple interacting oncogenes on the 8p11-p12 amplicon in human breast cancer. *Cancer Res.* 2006;66(24):11632–43.
42. Xie Z, Bailey A, Kuleshov MV, Clarke DJB, Evangelista JE, Jenkins SL, Lachmann A, Wojciechowicz ML, Kropiwnicki E, Jagodnik KM, et al. Gene set knowledge discovery with enrichr. *Curr Protoc.* 2021;1(3):e90.
43. Kuleshov MV, Jones MR, Rouillard AD, Fernandez NF, Duan Q, Wang Z, Koplev S, Jenkins SL, Jagodnik KM, Lachmann A, et al. Enrichr: a comprehensive gene set enrichment analysis web server 2016 update. *Nucleic Acids Res.* 2016;44(W1):W90–97.
44. Wang X, Spandidos A, Wang H, Seed B. PrimerBank: a PCR primer database for quantitative gene expression analysis, 2012 update. *Nucleic Acids Res.* 2012;40(Database issue):D1144–1149.
45. Untergasser A, Cutcutache I, Koressaar T, Ye J, Faircloth BC, Remm M, Rozen SG. Primer3—new capabilities and interfaces. *Nucleic Acids Res.* 2012;40(15):e115.
46. Lagarde N, Goldwasser E, Pencheva T, Jereva D, Pajeva I, Rey J, Tuffery P, Villoutreix BO, Miteva MA. A free Web-Based protocol to assist Structure-Based virtual screening experiments. *Int J Mol Sci.* 2019;20(18).
47. Lagarde N, Rey J, Gyulkhandanyan A, Tuffery P, Miteva MA, Villoutreix BO. Online structure-based screening of purchasable approved drugs and natural compounds: retrospective examples of drug repositioning on cancer targets. *Oncotarget.* 2018;9(64):32346–61.
48. Li Y, Dou Y, Da Veiga Leprevost F, Geffen Y, Calinawan AP, Aguet F, Akiyama Y, Anand S, Birger C, Cao S, et al. Proteogenomic data and resources for pan-cancer analysis. *Cancer Cell.* 2023;41(8):1397–406.
49. Walsh CT, Garneau-Tsodikova S, Gatto GJ Jr. Protein posttranslational modifications: the chemistry of proteome diversifications. *Angew Chem Int Ed Engl.* 2005;44(45):7342–72.
50. Hornbeck PV, Kornhauser JM, Latham V, Murray B, Nandhikonda V, Nord A, Skrzypek E, Wheeler T, Zhang B, Gnaf F. 15 Years of PhosphoSitePlus(R): integrating post-translationally modified sites, disease variants and isoforms. *Nucleic Acids Res.* 2019;47(D1):D433–41.
51. Urick ME, Bell DW. Clinical actionability of molecular targets in endometrial cancer. *Nat Rev Cancer.* 2019;19(9):510–21.
52. Setiawan VW, Yang HP, Pike MC, McCann SE, Yu H, Xiang YB, Wolk A, Wentzensen N, Weiss NS, Webb PM, et al. Type I and II endometrial cancers: have they different risk factors? *J Clin Oncol.* 2013;31(20):2607–18.
53. Cancer Genome Atlas Research N, Kandoth C, Schultz N, Cherniack AD, Akbani R, Liu Y, Shen H, Robertson AG, Pashtan I, Shen R, et al. Integrated genomic characterization of endometrial carcinoma. *Nature.* 2013;497(7447):67–73.
54. Bogani G, Ray-Coquard I, Concin N, Ngoi NYL, Morice P, Enomoto T, Takehara K, Denys H, Nout RA, Lorusso D, et al. Uterine serous carcinoma. *Gynecol Oncol.* 2021;162(1):226–34.
55. Howard TP, Vazquez F, Tsherniak A, Hong AL, Rinne M, Aguirre AJ, Boehm JS, Hahn WC. Functional genomic characterization of cancer genomes. *Cold Spring Harb Symp Quant Biol.* 2016;81:237–46.
56. Borowicz S, Van Scoyk M, Avasarala S, Karuppusamy Rathinam MK, Tauler J, Bikkavilli RK, Winn RA. The soft agar colony formation assay. *J Vis Exp.* 2014;(92):e51998.
57. Cockman E, Anderson P, Ivanov P. TOP mRNPs: molecular mechanisms and principles of regulation. *Biomolecules.* 2020;10(7).
58. Philippe L, van den Elzen AMG, Watson MJ, Thoreen CC. Global analysis of LARP1 translation targets reveals tunable and dynamic features of 5' TOP motifs. *Proc Natl Acad Sci U S A.* 2020;117(10):5319–28.
59. Huang ZH, Du YP, Wen JT, Lu BF, Zhao Y. SnoRNAs: functions and mechanisms in biological processes, and roles in tumor pathophysiology. *Cell Death Discov.* 2022;8(1):259.
60. O'Brien SJ, Fiechter C, Burton J, Hallion J, Paas M, Patel A, Patel A, Rochet A, Scheurlen K, Gardner S, et al. Long non-coding RNA ZFAS1 is a major regulator of epithelial-mesenchymal transition through miR-200/ZEB1/E-cadherin, vimentin signaling in colon adenocarcinoma. *Cell Death Discov.* 2021;7(1):61.
61. Rao M, Xu S, Zhang Y, Liu Y, Luan W, Zhou J. Long non-coding RNA ZFAS1 promotes pancreatic cancer proliferation and metastasis by sponging miR-497-5p to regulate HMGA2 expression. *Cell Death Dis.* 2021;12(10):859.
62. Wu H, Qin W, Lu S, Wang X, Zhang J, Sun T, Hu X, Li Y, Chen Q, Wang Y, et al. Long noncoding RNA ZFAS1 promoting small nucleolar RNA-mediated 2'-O-methylation via NOP58 recruitment in colorectal cancer. *Mol Cancer.* 2020;19(1):95.
63. Forli S, Huey R, Pique ME, Sanner MF, Goodsell DS, Olson AJ. Computational protein-ligand Docking and virtual drug screening with the AutoDock suite. *Nat Protoc.* 2016;11(5):905–19.
64. Fradera X, Babaoglu K. Overview of methods and strategies for conducting virtual small molecule screening. *Curr Protoc Chem Biol.* 2017;9(3):196–212.
65. Forli S. Charting a path to success in virtual screening. *Molecules.* 2015;20(10):18732–58.
66. Pettersen EF, Goddard TD, Huang CC, Couch GS, Greenblatt DM, Meng EC, Ferrin TE. UCSF Chimera—a visualization system for exploratory research and analysis. *J Comput Chem.* 2004;25(13):1605–12.
67. Garg G, Dienemann C, Farnung L, Schwarz J, Linden A, Urlaub H, Cramer P. Structural insights into human co-transcriptional capping. *Mol Cell.* 2023;83(14):2464–e24772465.
68. Li Y, Wang Q, Xu Y, Li Z. Structures of co-transcriptional RNA capping enzymes on paused transcription complex. *Nat Commun.* 2024;15(1):4622.
69. Bohnsack KE, Ficner R, Bohnsack MT, Jonas S. Regulation of DEAH-box RNA helicases by G-patch proteins. *Biol Chem.* 2021;402(5):561–79.
70. Feng Q, Krick K, Chu J, Burge CB. Splicing quality control mediated by DHX15 and its G-patch activator SUGP1. *Cell Rep.* 2023;42(10):113223.
71. Johnson JL, Yaron TM, Huntsman EM, Kerelsky A, Song J, Regev A, Lin TY, Liberatore K, Cizin DM, Cohen BM, et al. An atlas of substrate specificities for the human serine/threonine Kinome. *Nature.* 2023;613(7945):759–66.
72. Miller CJ, Turk BE. Homing in: mechanisms of substrate targeting by protein kinases. *Trends Biochem Sci.* 2018;43(5):380–94.
73. Dohnalkova M, Krasnykov K, Mendel M, Li L, Panasenko O, Fleury-Olela F, Vagbo CB, Homolka D, Pillai RS. Essential roles of RNA cap-proximal ribose methylation in mammalian embryonic development and fertility. *Cell Rep.* 2023;42(7):112786.
74. Yermalovich AV, Mohsenin Z, Cowdin M, Giotti B, Gupta A, Feng A, Golomb L, Wheeler DB, Xu K, Tsankov A, et al. An essential role for Cmtr2 in mammalian embryonic development. *Dev Biol.* 2024;516:47–58.
75. Lee YL, Kung FC, Lin CH, Huang YS. CMTR1-Catalyzed 2'-O-Ribose methylation controls neuronal development by regulating Camk2alpha expression independent of RIG-I signaling. *Cell Rep.* 2020;33(3):108269.

76. Simabuco FM, Pavan ICB, Pestana NF, Carvalho PC, Basei FL, Campos Granato D, Paes Leme AF, Zanchin NIT. Interactome analysis of the human Cap-specific mRNA (nucleoside-2'-O-)-methyltransferase 1 (hMTr1) protein. *J Cell Biochem.* 2019;120(4):5597–611.
77. Smith JC, Sheltzer JM. Genome-wide identification and analysis of prognostic features in human cancers. *Cell Rep.* 2022;38(13):110569.
78. Liu J, Lichtenberg T, Hoadley KA, Poisson LM, Lazar AJ, Cherniack AD, Kovatich AJ, Benz CC, Levine DA, Lee AV, et al. An integrated TCGA Pan-Cancer clinical data resource to drive High-Quality survival outcome analytics. *Cell.* 2018;173(2):400–16. e411.

Publisher's note

Springer Nature remains neutral with regard to jurisdictional claims in published maps and institutional affiliations.